ISSN: 2414-1895 DOI: 10.6919/ICJE.202306_9(6).0011

Study on the Failure Law of Cement Paste under the Combined Action of Cl-, SO_4^{2-} and Dry Wet Cycling

An Guo*

School of Materials and Science Engineering, Henan Polytechnic University, Jiaozuo Henan 45400, China

*2419884839@qq.com

Abstract

In order to investigate the damage law of cement slurry under the combined action of Cl^-, SO_4^{2-} and dry wet cycles, a NaCl-Na_2SO_4 composite solution was used to naturally soak and dry wet cycle corrode pure cement slurry, hardened Portland cement slurry with 30% fly ash and 30% mineral powder. The effects of SO_4^{2-} concentration (0.1mol/L, 0.5mol/L, 1.0mol/L) in environmental solution on the mechanical properties, corrosion product phase composition, and micro morphology of hardened Portland cement slurry were studied under natural immersion and dry wet cycling conditions with a fixed total chloride ion concentration of 0.6mol/L. The results show that under natural immersion and dry wet cycling conditions, the addition of mineral powder and fly ash to cement slurry under the coupling erosion of Cl^- and SO_4^{2-} is beneficial for resisting the erosion of Cl^- and SO_4^{2-}. At the same time, compared to natural immersion, under the dry wet cycling system, the strength of the test blocks in each erosion solution shows a decreasing trend and the strength loss rate is greater, which leads to more severe deterioration of their performance; Introducing SO_4^{2-} into an erosive environment where Cl^- exists, on the one hand, the diffusion rate of Cl^- is higher than that of SO_4^{2-}, which leads to a chemical reaction between Cl^- and hydration products to generate Friedel salts. On the other hand, due to the unfavorable effect of SO_4^{2-} on the existence of Friedel salts, the erosion of Cl^- and SO_4^{2-} interacts and constrains each other; Due to the introduction of SO_4^{2-}, combined with the release of chloride ions into the pore solution, the content of free chloride ions in the pore solution is increased; In a Na_2SO_4 solution with a high concentration (1.0mol/L), cement will be destroyed due to the superposition effect of physical crystallization and chemical erosion.

Keywords

Natural Soaking; Dry Wet Cycling; NaCl-Na_2SO_4; Microstructure; Ion Coupling Effect.

1. Introduction

Portland cement has become the largest and most important civil engineering building material in today's society, used to construct a large number of modern components and structures, and is widely used in various types of marine infrastructure construction. The application of a number of marine engineering projects such as cross sea bridges, port terminals, island and reef construction, underwater tunnels, offshore oil drilling platforms, and offshore floating structures is becoming increasingly widespread [1]. On the other hand, for cement slurries that have been exposed to marine environments for a long time, their service environment is harsh and complex. Given the high content of inorganic salts and various complex factors such as dry wet alternation in the marine environment. Long term service in corrosive environments has led to severe aging of many marine building

ISSN: 2414-1895 DOI: 10.6919/ICJE.202306_9(6).0011

structures, such as seaports and docks [2], dams [3], and bridges [4], before reaching their service life, requiring significant maintenance or reconstruction, and premature large-scale repairs [5,6]. Especially, the damage caused by chloride ion erosion seriously affects the service life of building structures. Therefore, the durability of components mainly composed of cement slurry largely determines the service life and structural integrity of these buildings [7-13]. The deterioration of cement slurry in the marine environment has become a key issue that needs to be urgently addressed at this stage. Therefore, the durability of cement slurry cannot be effectively solved, which will seriously constrain the rapid development of marine engineering construction in China. On the one hand, in-service cement slurry often suffers from harsh marine environments, and the mechanical properties (strength, elastic modulus, etc.) of cement slurry may significantly decrease over time. Ion erosion in seawater is one of the main reasons for material damage. Generally speaking, chloride ions enter the cement slurry quite slowly. But when the cement slurry comes into contact with seawater, due to the presence of many corrosive ions such as Cl^- and SO_4^{2-} in the seawater, the cement slurry will be damaged by the coupling effect of various ions, which will accelerate the entry of chloride ions and further deteriorate the interior of the cement slurry. Therefore, multiple ion coupling erosion will reduce the service life of cement slurry in marine environments. On the other hand, cement slurry exists in multiple erosion areas in the marine environment. According to the "Technical Specification for Anticorrosion of Concrete Structures in Port Engineering" (JTJ275-2000) standard, the service positions of port engineering can be mainly divided into underwater areas, tidal areas, atmospheric areas, and splash areas. Among them, cement slurry is most severely damaged by ion erosion in the marine tidal areas [14]. As the tide rises and falls in the ocean tidal zone, the cement slurry undergoes three alternating states, including seawater immersion state, wet state covered by seawater liquid film, and dry state [15]. When the tide rises, the exposed surface of cement slurry in the marine environment will be soaked by seawater; When the tide falls, the surface moisture of the cement slurry will evaporate, leading to the concentration of seawater located on the surface of the slurry, accelerating the entry of various ions into the pore solution inside the building components, and reducing its durability. At the same time, the concentration of inorganic salt ions in the tidal zone environment is higher than that in the immersion zone, and its concentration will also change. The complex and harsh tidal zone environment will lead to more severe erosion damage of cement slurry. There are multiple corrosive ions such as SO_4^{2-} and Cl^- present in the seawater of tidal zones, and there is mutual influence between these ions in terms of chemical erosion [16,17]. Given the high concentration of chloride ions in the marine environment, when chloride ions enter the interior of components and are transported to the surface of reinforced concrete reinforcement, the concentration of chloride ions reaches a certain threshold, causing damage to the passivation film on the surface of the reinforcement, leading to electrochemical corrosion and depassivation of the protective layer on the surface of the reinforcement [18], Therefore, most of the current research on the impact of seawater on cement slurry focuses on the corrosion of steel bars caused by chloride ions and the influence of different ions on the transport of Cl^- ions in cement slurry. The research on the corrosion mechanism of cement slurry under the coupling effect of multiple ions (SO_4^{2-}, Cl^-) in tidal environments is relatively unclear. Therefore, based on the above issues, this study conducts a study on the macro and micro structures of water slurry under the coupling action of multiple ions (SO_4^{2-}, Cl^-) in tidal environments (divided into natural immersion and dry wet cycling). The research results can provide theoretical support for the development of anti-corrosion technologies for building components mainly composed of cement slurry in marine environments and the durability design of high corrosion resistant building materials

2. Test

2.1 Raw Materials

The experimental materials were fly ash (FA) produced by Gongyi Longze Water Purification Materials Co., Ltd. and ground granulated blast furnace slag (GGBS) produced by Gongyi Longze Water Purification Materials Co, Ltd. The Portland cement used in the experiment was produced by

ISSN: 2414-1895 DOI: 10.6919/ICJE.202306_9(6).0011

Jiaozuo Qianye Cement Co, Ltd. Its chemical composition and physical and mechanical properties are shown in Tables 1 and 2. The mineral composition and content of Portland cement are shown in Table 3. The chemical composition of fly ash and mineral powder is shown in Table 4. Fly ash is industrial solid waste discharged from fossil-fuel power station, which has micro aggregate effect and chemical activity effect. Mineral powder is a powder material obtained by grinding the slag discharged from an ironmaking blast furnace after quenching and quenching with water. The design of cement paste mix proportion is shown in Table 5.

Table 1. Chemical Composition of Portland Cement (wt.%)

Oxide	SiO_2	Al_2O_3	Fe_2O_3	CaO	MgO	SO_3	Na_2O	f-CaO	Cl^-	LOI
Content	21.192	5.03	3.38	63.32	2.01	2.06	0.55	0.68	0.018	1.76

Table 2. Physical Properties of Portland Cement

Fineness(0.08/%)	Density(g/cm^3)	Specific surface area(m^2/Kg)	Standard consistency(%)	setting time(min)	
				Initial setting	Final set
0.4	3.12	354	24.60	95	155

Table 3. Mineral Composition Content of Portland Cement (wt.%)

Mineral	C_3S	C_2S	C_3A	C_4AF	other
Content	57.55	17.82	7.54	11.19	5.9

Table 4. Chemical composition of fly ash and blast furnace slag (data presented by mass %)

Mineral	CaO	SiO_2	Al_2O_3	Fe_2O_3	SO_3	MgO	Na_2O	LOI
FA	7.26	50.26	33.14	4.16	2.16	0.23	0.45	2.34
GGBS	34.00	36.56	17.70	1.03	1.64	8.01	0.22	0.84

2.2 Specimen Forming and Curing

Forming water cement ratio 0.4, specimen size 70mm × 70mm × 70mm, several demoulded slurry specimens were prepared according to the standard GB/T1346-2011 "Testing Methods for Water, Setting Time, and Stability of Cement Standard Consistency" after 24 hours. They were placed in a wet curing room and maintained for 28 days to eliminate the impact of imminent erosion at the aggregate interface. Place the hardened cement slurry that has been cured for 28 days in a constant temperature room for erosion immersion, with a solid-liquid mass ratio of 1:20. Some of the specimens were subjected to natural immersion erosion, while the remaining 5 surfaces were sealed with epoxy resin and then subjected to dry wet cyclic immersion erosion. According to relevant literature, this experiment adopts a natural soaking time of 90 days, a dry wet cycle system of 16 hours of soaking, and a drying cycle of 8 hours, with a total of 40 cycles. At the same time, in order to simulate the ion concentration in the tidal zone environment and accelerate the experimental process, it is recommended to choose SO_4^{2-} ion concentration from three corrosion solutions with gradients of 0.1mol/L, 0.5mol/L, and 1.0mol/L. The specific proportion of ion concentration in the corrosion solution is shown in Table 5, and a total of 10 sets of corrosion solution environments were designed. The focus is on studying the failure mechanism of cement slurry under the coupling effect of the same Cl^- concentration and different SO_4^{2-} concentrations.

ISSN: 2414-1895 DOI: 10.6919/ICJE.202306_9(6).0011

Table 5. Concentration of exposed solutions used in the experiment

Concentration of exposed solutions	Chloride ion (mol/L)	Magnesium Concentration (mol/L)	Abbreviation
0.6mol/L NaCl	0.6	-	0.6NC
0.6mol/L NaCl+0.1mol/L Na_2SO_4	0.6	0.1	0.4NC-0.1NS
0.6mol/L NaCl+0.5mol/L Na_2SO_4	0.6	0.5	0.2NC-0.2NS
0.6mol/L NaCl+1.0mol/L Na_2SO_4	0.6	1.0	0.0NC-0.3NS

2.3 Test Methods

The cement slurry is evenly mixed by a mixer at a depth of 70mm × 70mm × The 70mm test mold is poured into shape and cured in a curing room (temperature 20 ± 2 ℃, relative humidity ≥ 90%). After 24 hours of curing, the mold is demolded and a portion of the test blocks are soaked in 10 different corrosion solutions to fully immerse and corrode them. The natural soaking time is about 90 days; The remaining test blocks in the dry wet cycle are soaked and eroded for 16 hours in the dry wet cycle system, and dried in a drying oven for 8 hours for a total of 40 cycles. After curing to the corresponding age, compressive strength tests are carried out using the YAW-300/20 microcomputer controlled fully automatic pressure testing machine produced by Shanghai Bairuo Testing Instrument Co., Ltd. The test is carried out using displacement loading method, and the test is conducted every hour during the test process, The loading speed is 1mm/min. Conduct compressive strength tests in each erosion environment, with 3 blocks in each group. The average of the final test results is taken as the compressive strength of the above 3 blocks. Thermogravimetric analysis: Place the soaked sample in a 40 ℃ vacuum drying oven for 3 days, and use the HCT-3 microcomputer differential thermal balance produced by Beijing Science Instrument Factory to test and analyze the prepared sample. The temperature range for testing is 25~500 ℃, and the heating rate is 10 ℃/min. X-ray diffraction analysis: The X-ray diffractometer produced by Dandong Haoyuan Co, Ltd, manufactured in China, was used for testing and analysis, and the obtained samples were characterized for phase composition. Cu target and K were used in the experiment α Radiation, tube voltage 40KV, tube current 150mA, scanning area 5-70 °, scanning speed 5 °/min. When electrons impact a material, they undergo a series of elastic and non elastic collisions with atoms in the material. By using different signal detectors in the microscope to detect the signals generated by these collisions (secondary electrons, backscattered electrons, and characteristic X-rays), relevant information such as the morphology and composition of the tested sample itself, the cutting thickness of 5mm, etc., can be obtained by cutting the test block from its surface after natural soaking and dry wet cycling using a cutting machine. Among them, starting from its unsealed surface, the test block subjected to dry wet cycling is cut. The obtained sample was dried in a 40 degree vacuum oven for 72 hours, and finally ground into powder using a three head grinder. It was then sieved through a 200 mesh sieve to stop the hydration of the obtained particles in alcohol. After vacuum deposition gold spraying treatment, the particle sample was observed with a scanning electron microscope of MERLIN Compact model from Carl Zeiss, Germany, and the composition of the observed microstructure was analyzed with a Bruker Quantax200 XFlash energy spectrometer.

3. Results and Discussion

3.1 The Influence of SO_4^{2-} on the Destruction Law of Cement Slurry under Natural Soaking and Dry Wet Cycling

3.1.1 Compressive Strength of Cement Slurry under Natural Immersion in Cl--SO_4^{2-} Erosive Environment

The compressive strength changes of cement paste specimens in various corrosive solutions under natural immersion are shown in Figure 1. Compared with the compressive strength of cement slurry specimens of the same system in various dissolution solutions, it is not difficult to find that the compressive strength of pure water slurry specimens increases with the increase of SO_4^{2-}

ISSN: 2414-1895 DOI: 10.6919/ICJE.202306_9(6).0011

concentration in the dissolution solution when Cl^- and SO_4^{2-} are coupled. At the same time, it was found that the compressive strength of the slurry containing mineral admixtures in an erosion solution of 0.6mol/L Cl^--1.0mol/L SO_4^{2-} slightly decreased compared to that in an erosion solution of 0.6mol/L Cl^--0.5mol/L SO_4^{2-}. In addition, the compressive strength of pure water slurry showed a decreasing trend after the introduction of SO_4^{2-} in the presence of Cl^- erosion solution, with a strength loss rate of 28.8%. However, the slurry of mineral admixture system showed an increasing trend after the introduction of SO_4^{2-} in the presence of Cl^- erosion solution. The compressive strength of cement fly ash system increased by 18.2%, and the compressive strength of cement mineral powder system increased by 15.1%.

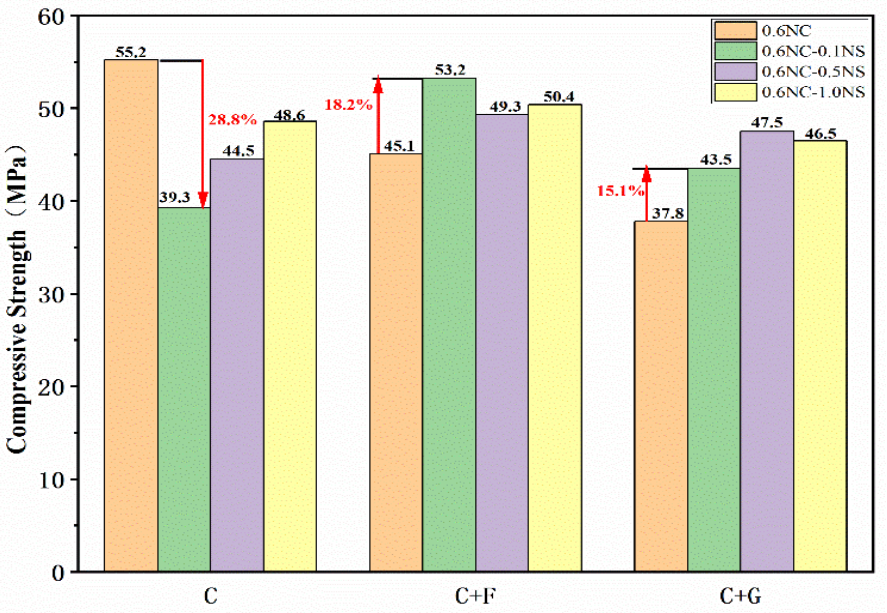

Figure 1. Compressive strength of cement slurry under natural immersion for 90d in Cl^--SO_4^{2-} erosion environment

3.1.2 Compressive Strength of Cement Slurry under Dry Wet Cycling in Cl--SO_4^{2-} Erosive Environment

The compressive strength changes of cement paste specimens in various corrosive solutions under dry wet cycles are shown in Figure 2. Compared to the compressive strength of cement paste specimens in various corrosive solutions of the same system, it is not difficult to find that the compressive strength of pure cement paste specimens increases with the increase of SO_4^{2-} concentration in the corrosive solution under the coupling of Cl^- and SO_4^{2-}. At the same time, it was found that the compressive strength of the slurry containing mineral admixtures in an erosion solution of 0.6mol/L Cl^-1.0mol/L SO_4^{2-} slightly decreased compared to that in an erosion solution of 0.6mol/L Cl^--0.5mol/L SO_4^{2-}. In addition, the compressive strength of pure water slurry showed a decreasing trend after the introduction of SO_4^{2-} in the presence of Cl^- erosion solution, with a strength loss rate of 43.7%, while the slurry of mineral admixture system showed an increasing trend after the introduction of SO_4^{2-} in the presence of Cl^- erosion solution. The compressive strength loss rate of cement fly ash system was 18.8%, and the compressive strength loss rate of cement mineral powder system was 12.2%. When the concentration of SO_4^{2-} in the erosion solution increases to 1.0mol/L, the compressive strength loss rate is greater; Compared to natural immersion, the strength of the test blocks in each erosion solution shows a decreasing trend under the dry wet cycle system, and the strength loss rate is greater, which has a greater impact on their performance degradation.

ISSN: 2414-1895 DOI: 10.6919/ICJE.202306_9(6).0011

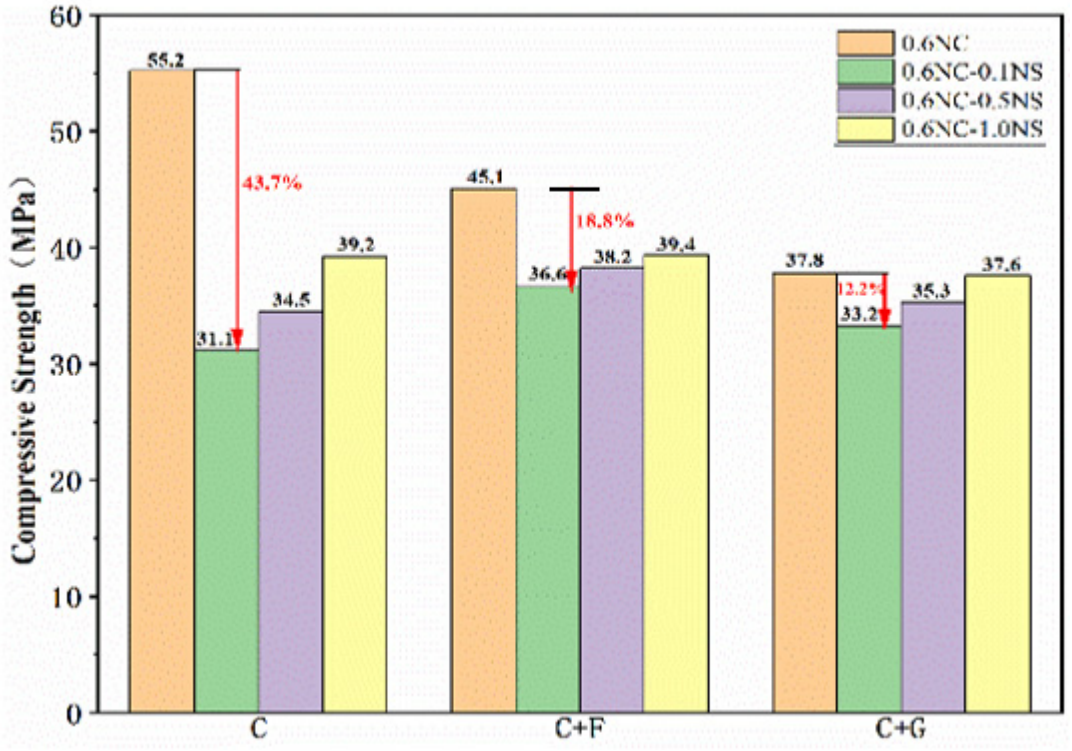

Figure 2. Compressive strength of cement slurry in Cl^--SO_4^{2-}erosion environment after drying and wetting for 40 days

3.1.3 Corrosion Products of Cement Slurry under Natural Soaking in Cl--SO_4^{2-} Erosion Environment

Figure 3 shows the phase composition of water slurry under different erosion solutions under natural immersion. The main phase composition of cement slurry in pure NaCl corrosive solution includes $Ca(OH)_2$; Friedel salt; The main phase composition of cement slurry in NaCl-Na_2SO_4 erosion solution includes $Ca(OH)_2$, Friedel salt, and gypsum. The introduction of different concentrations of SO_4^{2-} in the corrosive solution with Cl^- resulted in a decrease or even disappearance of Friedel salt diffraction peak intensity, indicating that the introduction of SO_4^{2-} in the corrosive solution with Cl^- was not conducive to the existence of Friedel salt.

Figure 3 (a) shows the XRD patterns of pure cement system samples after natural immersion in different erosion solutions for 90 days. From Figure 3 (a), it can be observed that compared with the erosion solution of a single Cl^-, the diffraction peak of Friedel salt in the sample significantly weakened and almost disappeared after the introduction of $SO4^{2-}$ in the erosion solution with Cl^-; When the concentration of SO_4^{2-} in the erosion solution reaches 1.0mol/L, the Friedel salt diffraction peak intensity does not change much compared to the diffraction peak intensity when the SO_4^{2-} concentration in the erosion solution is 0.1mol/L; In addition, compared to the erosion solution with a single Cl^-, the introduction of SO_4^{2-} in the erosion solution with Cl^- resulted in a decrease in the diffraction peak intensity of $Ca(OH)_2$ in the sample, and a dihydrate gypsum diffraction peak also appeared in the erosion product, but its diffraction peak intensity was not high. Figure 3 (b) shows the XRD patterns of the cement fly ash material system sample after natural immersion in different erosion solutions for 90 days. From Figure 3 (b), it can be observed that compared with the erosion solution of a single Cl^-, the diffraction peak of Friedel salt in the sample significantly weakened after the introduction of SO_4^{2-} in the erosion solution with Cl^-, and the diffraction peak intensity did not change significantly in the erosion solution with different SO_4^{2-} concentrations; In addition, compared to the erosion solution with a single Cl^-, the introduction of SO_4^{2-} in the erosion solution with Cl^- resulted in a decrease in the diffraction peak intensity of $Ca(OH)_2$ in the sample, and a dihydrate gypsum diffraction peak also appeared in the erosion product, but its diffraction peak intensity was not high. Figure 3 (c) shows the XRD patterns of the cement mineral powder material system sample

ISSN: 2414-1895 DOI: 10.6919/ICJE.202306_9(6).0011

after natural immersion in different erosion solutions for 90 days. From Figure 3 (c), it can be observed that compared to the erosion solution with a single Cl^-, the diffraction peak of Friedel salt in the sample significantly weakened after the introduction of SO_4^{2-} in the erosion solution with Cl^-, and the diffraction peak intensity did not change significantly in the erosion solution with different concentrations of SO_4^{2-}.

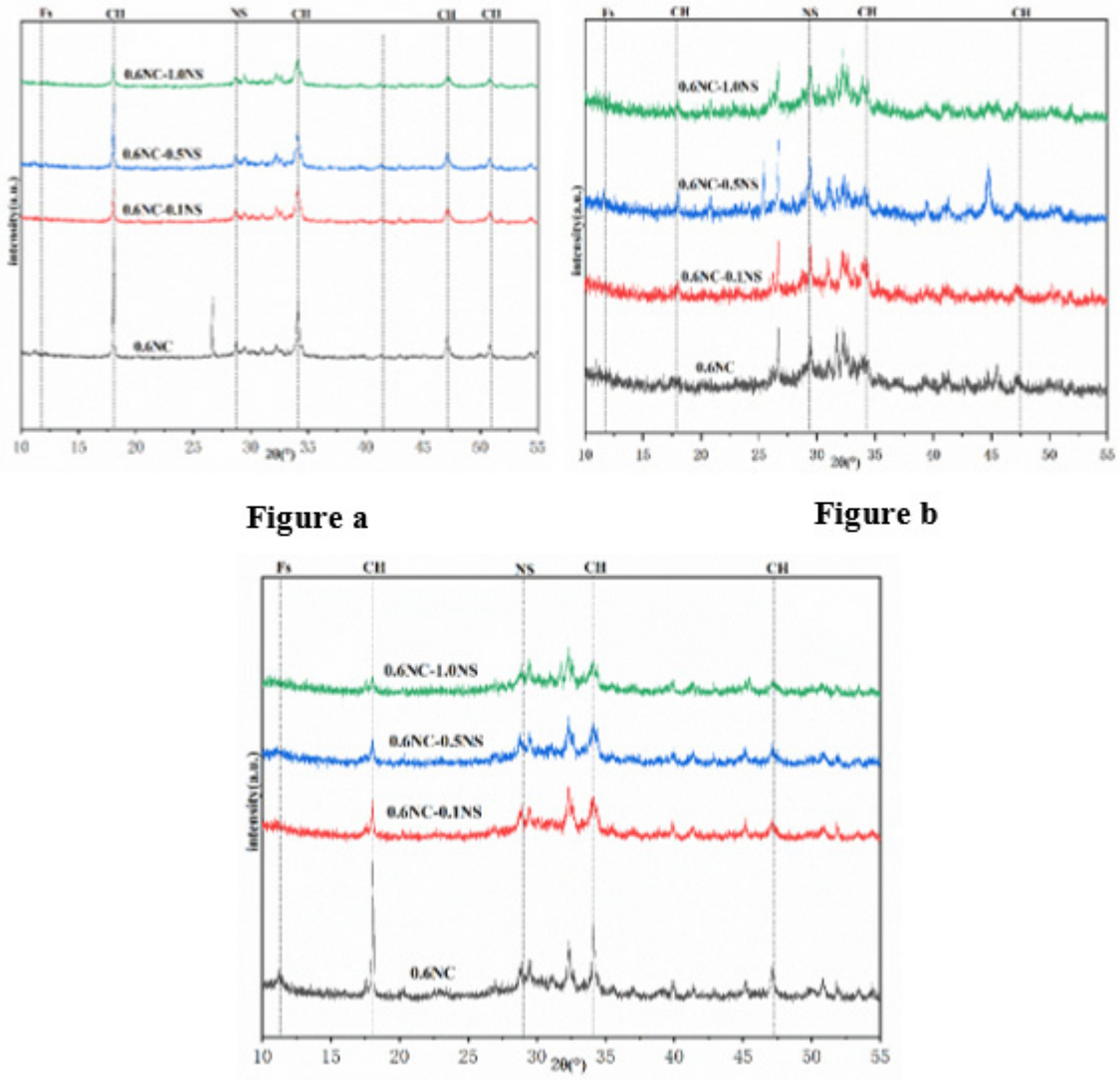

Figure a Figure b

Figure 3. XRD pattern of cement slurry after dry and wet cycling for 90d in Cl^--SO_4^{2-} erosion environment. (a) C; (b) C+F; (c) C+G

Under natural immersion, the changes in phase composition of cement slurry after 90 days of natural immersion in Cl^--SO_4^{2-} erosive solution can be determined through thermogravimetric testing. Figure 4 shows the DTG curve of cement slurry after 90 days of natural immersion in Cl^--SO_4^{2-} erosive solution. It can be seen from Figure 4 that there are several obvious endothermic peaks in the DTG curve after being eroded by cement slurry, of which the peak between 60 ℃ and 130 ℃ is mainly produced by dehydration of C-S-H gel [19], and the peak between 60 ℃ and 130 ℃ for cement slurry in Cl^--SO_4^{2-} erosion solution is produced by dehydration of C-S-H gel; The endothermic peak of 250 ℃ -350 ℃ belongs to Friedel salt [19], and the endothermic peak of 350 ℃ -420 ℃ belongs to $Mg(OH)_2$. The endothermic peak of 420 ℃ -520 ℃ belongs to $Ca(OH)_2$ [19]. According to the variation characteristics of the DTG curve of cement slurry after natural immersion in Cl^--SO_4^{2-} erosive solution for 90 days in Figure 4, it can be seen that the variation pattern of cement slurry for cement,

ISSN: 2414-1895 DOI: 10.6919/ICJE.202306_9(6).0011

cement fly ash, and cement mineral powder is similar with the increase of SO_4^{2-} concentration in the erosive solution.

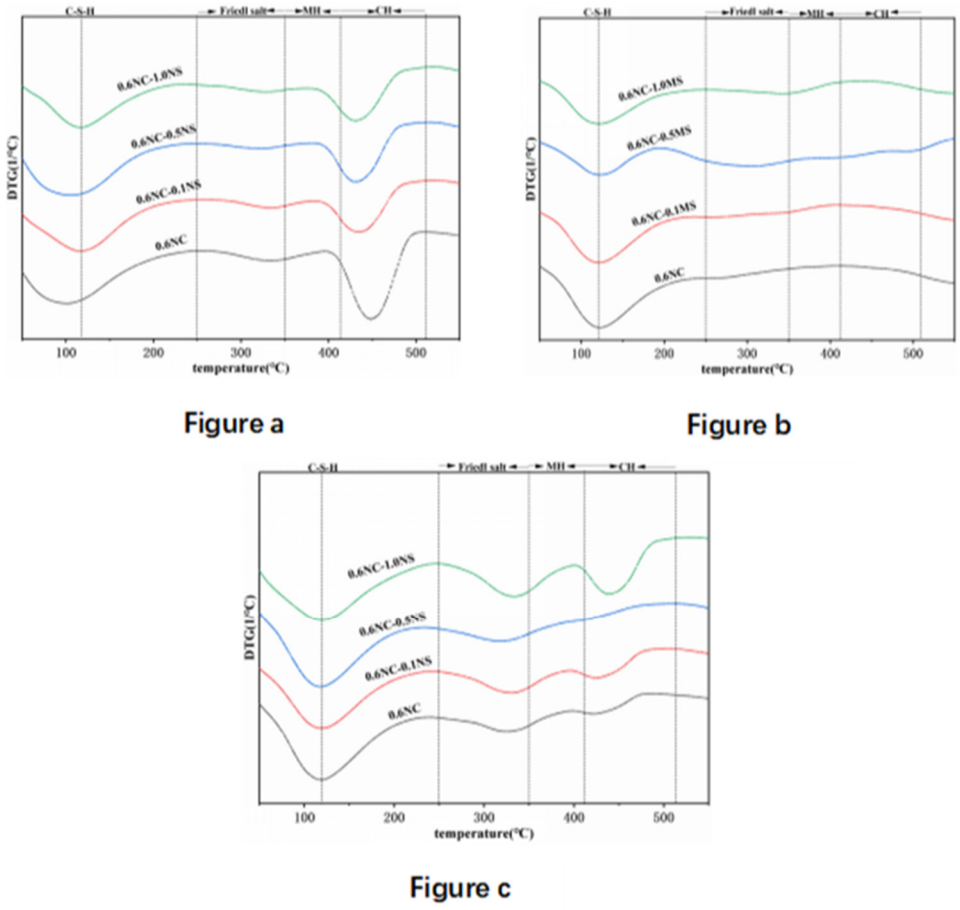

Figure 4. DTG spectrum of portland cement slurry soaked in CI-SO_4^2 erosive enviroment for 90 days. (a) C; (b)C+F; (c)C+G

3.1.4 Corrosion Products of Cement Slurry under Dry Wet Cycle in Cl--SO_4^{2-} Erosion Environment

Figures 5 show the phase composition of water slurry under different erosion solutions under dry wet cycles. The main phase composition of cement slurry in pure NaCl corrosive solution includes $Ca(OH)_2$; Friedel salt; The main phase composition of cement slurry in NaCl-Na_2SO_4 erosion solution includes $Ca(OH)_2$, Friedel salt, and gypsum. The introduction of different concentrations of SO_4^{2-} in the corrosive solution with Cl^- resulted in a decrease or even disappearance of Friedel salt diffraction peak intensity, indicating that the introduction of SO_4^{2-} in the corrosive solution with Cl^- was not conducive to the existence of Friedel salt. Figure 5 (a) shows the XRD patterns of pure cement system samples after 40 days of dry wet cycling in different erosion solutions. From Figure 5 (a), it can be observed that compared with the erosion solution of a single Cl^-, the diffraction peak of Friedel salt in the sample significantly weakened and almost disappeared after the introduction of SO_4^{2-} in the erosion solution of Cl^-; When the concentration of SO_4^{2-} in the erosion solution reaches 1.0mol/L, the Friedel salt diffraction peak intensity does not change much compared to the diffraction peak intensity when the SO_4^{2-} concentration in the erosion solution is 0.1mol/L; In addition, compared to the erosion solution with a single Cl^-, the introduction of SO_4^{2-} in the erosion solution with Cl^- resulted in a decrease in the diffraction peak intensity of $Ca(OH)_2$ in the sample, and a dihydrate gypsum diffraction peak also appeared in the erosion product, but its diffraction peak intensity was not high. Figure 5 (b) shows the XRD patterns of the cement fly ash material system samples after 40 days of dry wet cycling in different erosion solutions. From Figure 5 (b), it can be observed that compared to the erosion solution with a single Cl^-, the diffraction peak of Friedel salt in the sample is significantly weakened after the introduction of SO_4^{2-} in the erosion solution with Cl^-, and the diffraction peak

ISSN: 2414-1895 DOI: 10.6919/ICJE.202306_9(6).0011

intensity does not change significantly in the erosion solution with different SO_4^{2-} concentrations; In addition, compared to the erosion solution with a single Cl^-, the introduction of SO_4^{2-} in the erosion solution with Cl^- resulted in a decrease in the diffraction peak intensity of $Ca(OH)_2$ in the sample, and a dihydrate gypsum diffraction peak also appeared in the erosion product, but its diffraction peak intensity was not high.Figure 5 (c) shows the XRD patterns of the cement mineral powder material system samples after 40 days of dry wet cycling in different erosion solutions. From Figure 5 (c), it can be observed that compared to the erosion solution with a single Cl^-, the diffraction peak of Friedel salt in the sample significantly weakens after the introduction of SO_4^{2-} in the erosion solution with Cl^-, and the diffraction peak intensity does not change significantly in the erosion solution with different SO_4^{2-} concentrations; In addition, compared to the erosion solution with a single Cl^-, the introduction of SO_4^{2-} in the erosion solution with Cl^- resulted in a decrease in the diffraction peak intensity of $Ca(OH)_2$ in the sample, and a dihydrate gypsum diffraction peak also appeared in the erosion product, but its diffraction peak intensity was not high.

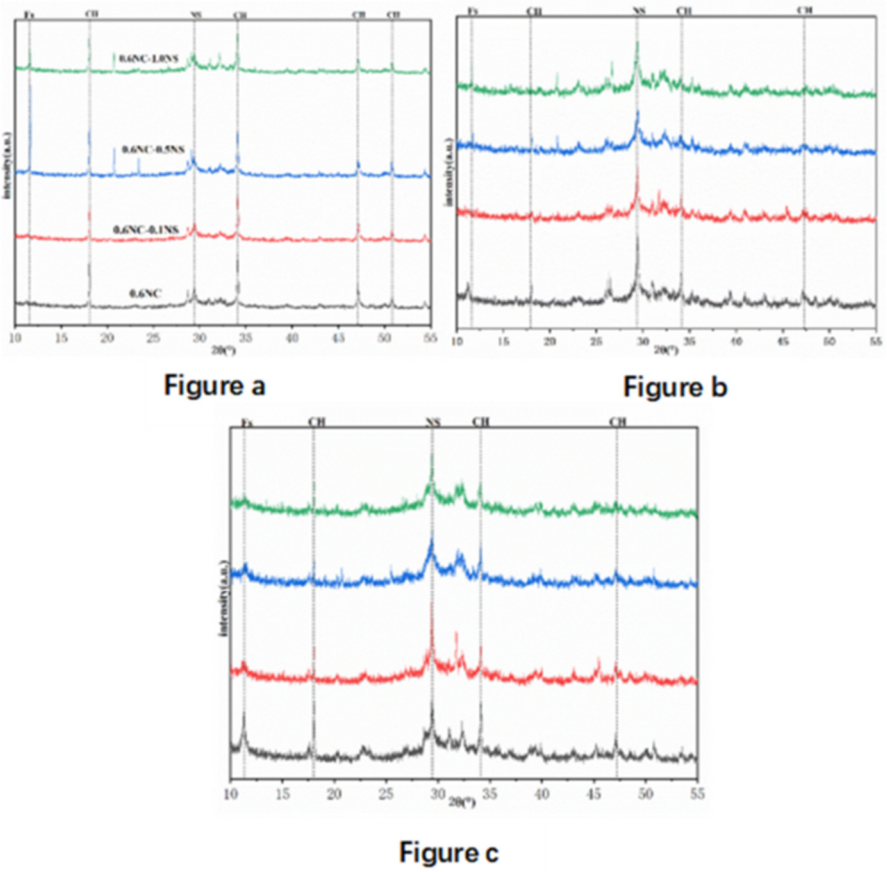

Figure 5. XRD pattern of cement slurry after dry and Wet cycling for 40d in CI-SO_4^2 erosion enviroment. (a) C; (b)C+ F; (c) C+G

Under the dry wet cycle, it can be seen through thermogravimetric testing that the phase composition of cement slurry changes after 40 days of dry wet cycle in Cl^--SO_4^{2-} erosive solution. Figure 6 shows the DTG curve of cement slurry after 40 days of dry wet cycle in Cl^--SO_4^{2-} erosive solution. It can be seen from Figure 6 that there are several obvious endothermic peaks in the DTG curve of cement slurry after erosion, of which the peak between 60 ℃ and 130 ℃ is mainly caused by the dehydration of C-S-H gel 19], and the peak between 60 ℃ and 130 ℃ for the cement slurry in Cl^-- SO_4^{2-} erosion solution is caused by the dehydration of C-S-H gel; The endothermic peak of 250 ℃ -350 ℃ belongs to Friedel salt [19], and the endothermic peak of 350 ℃ -420 ℃ belongs to $Mg(OH)_2$. The endothermic peak of 420 ℃ -520 ℃ belongs to $Ca(OH)_2$ [19]. According to the variation characteristics of the DTG curve of cement slurry in Cl^--SO_4^{2-} erosive solution after 40 days of dry

ISSN: 2414-1895 DOI: 10.6919/ICJE.202306_9(6).0011

wet cycling in Figure 6, it can be seen that the variation pattern of cement slurry for cement, cement fly ash, and cement mineral powder is similar with the increase of SO_4^{2-} concentration in the erosive solution.

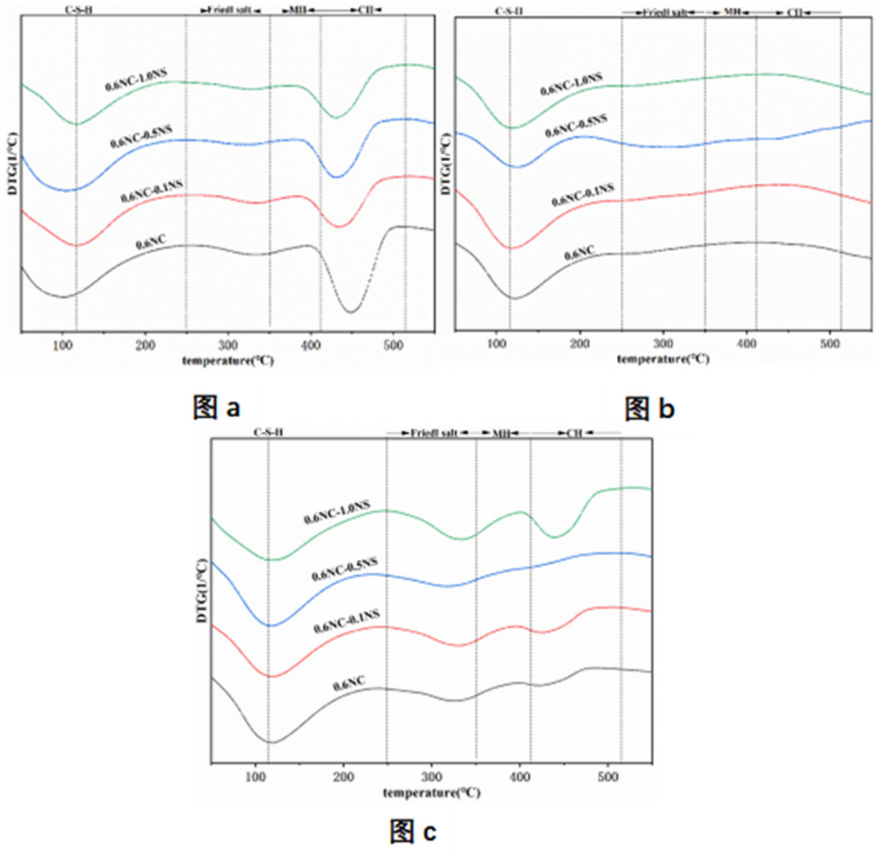

Figure 6. DTG diagram of portland cement slurry after drying and wetting for 40 davs in CI-SO_4^2 erosion enviroment. (a) C; (b)C+F; (c)C+ G

3.2 Microstructure of Cement Slurry in Cl--SO_4^2- Erosive Environment

3.2.1 Microscopic Morphology of Cement Slurry under Natural Immersion in Cl--SO_4^2- Erosive Environment

Figure 7 (a) shows the scanning electron microscope picture of pure cement slurry under the erosion environment of 0.6mol/L NaCl. It can be found that the hydration products are very rich, the needle bar shaped material is ettringite, the hexagonal plate shaped material is Friedel salt, and other plate shaped materials are calcium hydroxide; Figure 7 (b) shows the scanning electron microscope image of pure cement slurry under the corrosion environment of 0.6mol/L NaCl-0.1mol/L Na_2SO_4. It is not difficult to find needle like substances on its surface through scanning electron microscopy images. Through the analysis of energy spectrum elements, it is found that the elements existing in the needle bar material area mainly include Ca, Al, S and O, so it can be considered that the needle bar material existing in the area is ettringite. The cement slurry is immersed in the environment containing sodium sulfate and chloride, resulting in a lot of ettringite adhering to the surface of the cement slurry. On the other hand, no corrosion product gypsum was found, and no obvious deterioration was observed on the material surface, so there was a large amount of ettringite in the area without gypsum; Kunther et al. [20] found that there were a large number of ettringite and gypsum in the cement slurry immersed in a single sodium sulfate corrosive environment, and at the same time, it was observed by scanning electron microscope that the surface of the material was significantly deteriorated, so only when ettringite and gypsum existed at the same time would sodium sulfate corrosion damage occur.

ISSN: 2414-1895 DOI: 10.6919/ICJE.202306_9(6).0011

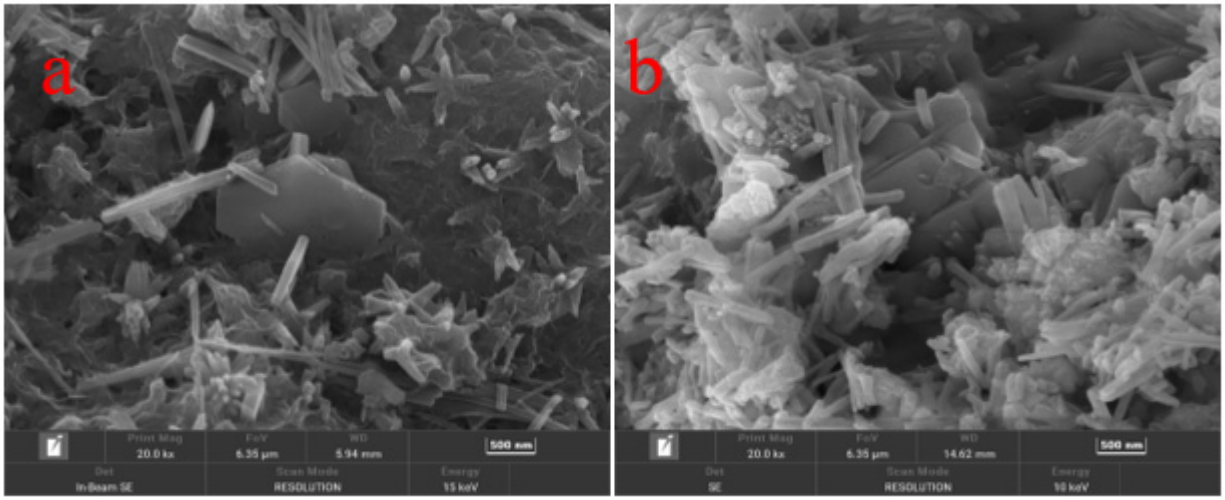

Figure 7. SEM EDS diagram of pure cement system sample after natural immersion in Cl^--SO_4^{2-} erosion solution for 90 days: (a) SEM diagram under 0.6mol/L NaCl erosion solution; (b) Scanning electron micrograph under the corrosive environment of 0.4mol/L NaCl-0.1mol/L Na_2SO_4

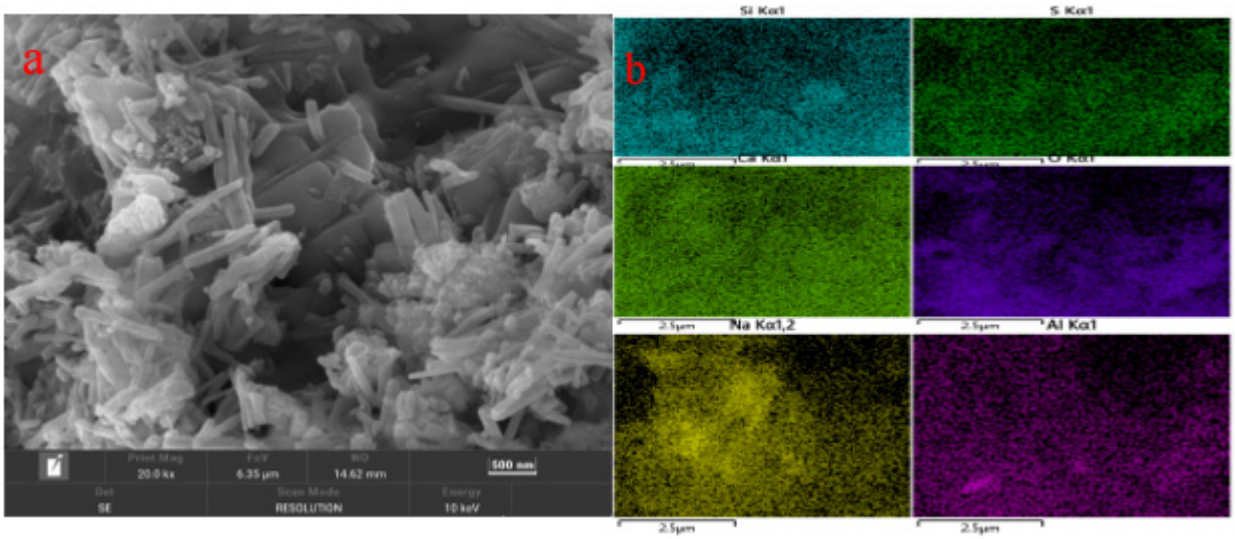

Figure 8. (a) shows the SEM-EDS diagram of pure cement slurry after natural immersion in 0.6mol/L NaCl-0.1mol/L Na_2SO_4 erosion solution for 90 days, and Figure (b) shows the energy spectrum surface scan diagram of Figure (a)

Figures 8 (a) show the scanning electron microscopy images of pure cement system samples after natural immersion in a 0.6mol/L NaCl-0.1mol/L Na_2SO_4 corrosive environment for 90 days. It is not difficult to find needle like substances on its surface through scanning electron microscopy images. Through the analysis of energy spectrum elements, it is found that the elements existing in the needle bar material area mainly include Ca, Al, S and O, so it can be considered that the needle bar material existing in the area is ettringite. The cement slurry is immersed in the environment containing sodium sulfate and chloride, resulting in a lot of ettringite adhering to the surface of the cement slurry. On the other hand, no corrosion product gypsum was found, and no significant deterioration was observed on the material surface.

3.2.2 Microscopic Morphology of Cement Slurry under Dry Wet Cycling in Cl--SO_4^{2-} Erosive Environment

Figure 9 (a) shows the scanning electron microscope picture of pure cement slurry under the erosion environment of 0.6mol/L NaCl. It can be found that the hydration products are very rich, the needle

ISSN: 2414-1895 DOI: 10.6919/ICJE.202306_9(6).0011

bar shaped material is ettringite, the hexagonal plate shaped material is Friedel salt, and other plate shaped materials are calcium hydroxide; Figures 9 (b) show the scanning electron microscope images of pure cement slurry under the corrosion environment of 0.6mol/L NaCl-0.1mol/L Na_2SO_4. Through the scanning electron microscope images, it is not difficult to find that its hydration products contain a large amount of needle like substances, but substances with regular morphology have not been found. This further indicates that the Friedel salt content is low and the ettringite content is increased after the introduction of SO42 - in a single chloride environment. Due to the erosion of sulfate, Friedel salt is converted into AFt, which will lead to the imbalance of chemical binding of chloride ions

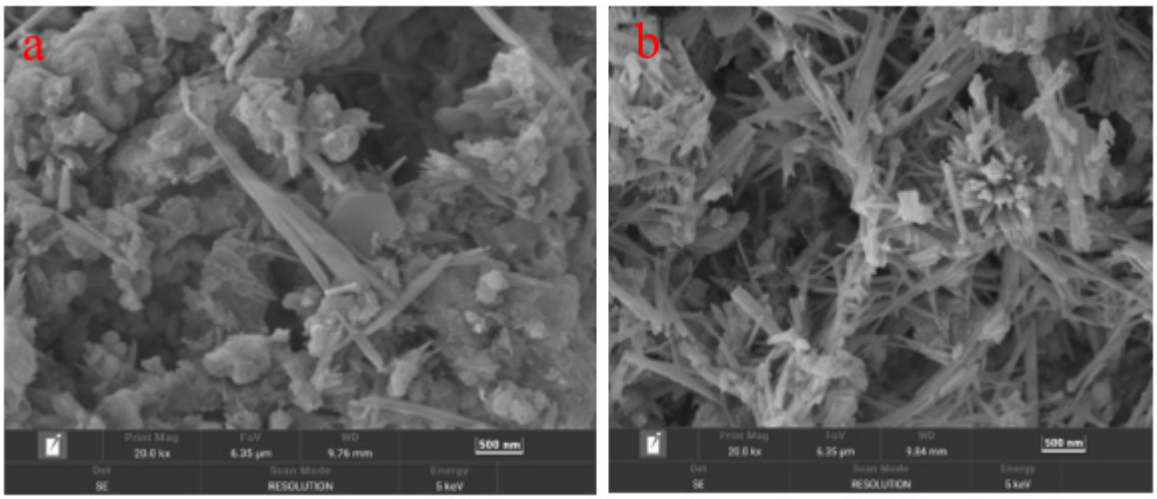

Figure 9. SEM-EDS diagram of pure cement system sample after drying and wetting in Cl^--SO_4^{2-} corrosion solution for 40 days: (a) SEM diagram under 0.6mol/L NaCl corrosion solution; (b) Scanning electron micrograph under the corrosive environment of 0.6mol/L NaCl-0.1mol/L Na_2SO_4

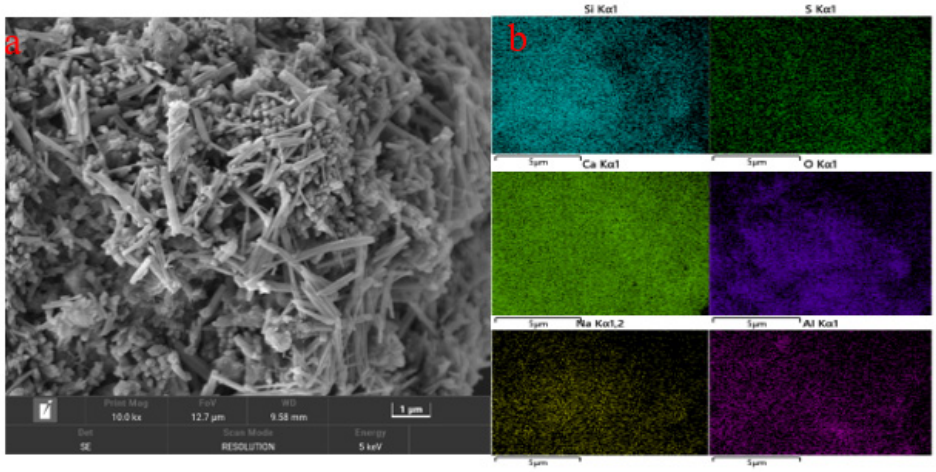

Figure 10. (a) shows the SEM-EDS diagram of pure cement slurry after 40 days of dry wet cycling in a 0.6mol/L NaCl-0.1mol/L Na_2SO_4 erosive solution, and Figure (b) shows the energy spectrum surface scan of Figure (a)

Figures 10 (a) show the scanning electron microscopy images of pure cement system samples after 40 days of dry wet cycling in a 0.6mol/L NaCl-0.1mol/L Na_2SO_4 corrosive environment. It is not difficult to find needle like substances on its surface through scanning electron microscopy images. Through the analysis of energy spectrum elements, it is found that the elements existing in the needle bar material area mainly include Ca, Al, S and O, so it can be considered that the needle bar material existing in the area is ettringite. The cement slurry is immersed in the environment containing sodium sulfate and chloride, resulting in a lot of ettringite adhering to the surface of the cement slurry. On

ISSN: 2414-1895 DOI: 10.6919/ICJE.202306_9(6).0011

the other hand, no corrosion product gypsum was found, and no obvious deterioration was observed on the material surface, so there was a large amount of ettringite in the area without gypsum; Kunther et al.[20] found that there were a large number of ettringite and gypsum in the cement slurry immersed in a single sodium sulfate corrosive environment, and at the same time, it was observed by scanning electron microscope that the surface of the material was significantly deteriorated, so only when ettringite and gypsum existed at the same time would sodium sulfate corrosion damage occur.

4. Conclusion

(1) In the environment of natural immersion and dry wet cycling, the addition of mineral powder and fly ash to cement slurry under the coupling erosion of Cl^- and SO_4^{2-} is beneficial for resisting the erosion of Cl^- and SO_4^{2-}. At the same time, compared to natural immersion, under the dry wet cycling system, the strength of the test blocks in each erosion solution shows a downward trend and the strength loss rate is greater, which leads to more severe deterioration of their performance.

(2) In the environment of natural immersion and dry wet cycling, SO_4^{2-} is introduced into the corrosive environment where Cl^- exists. On the one hand, the diffusion rate of Cl^- is higher than that of SO_4^{2-}, which leads to the chemical reaction between Cl^- and hydration products to generate Friedel salts. On the other hand, due to the unfavorable effect of SO_4^{2-} on the existence of Friedel salts, the erosion of Cl^- and SO_4^{2-} interacts and constrains each other; Due to the introduction of SO_4^{2-}, combined with the release of chloride ions into the pore solution, the content of free chloride ions in the pore solution is increased.

(3) Under natural immersion and dry wet cycling, SO_4^{2-} and Cl^- in the erosion solution react with the hydration products of the matrix. In an environment with a high concentration of Na_2SO_4 erosion solution (1.0mol/L), the cement slurry will be destroyed by physical crystallization and chemical erosion of the salt solution.

References

[1] Yuan Yingshu. Durability Design, Evaluation and Test of Reinforced Concrete Structures [M]. China University of Mining and Technology Press, 2013.

[2] Wang Shengnian, Huang Junzhe, Zhang Julian, Pan Deqiang. Investigation on Concrete corrosion and structural durability analysis of South China Port [J]. Water Transport Engineering, 2000, 6: 8-12.

[3] He Wen. Investigation and study on dissolution erosion of large and medium-sized reservoir DAMS in Jiangxi Province [D]. Nanchang: Nanchang University, 2015.

[4] Hong Naifeng. Corrosion and life economic analysis of reinforced concrete infrastructure [J]. Building Technology, 2002, 33(4): 254-257. (in Chinese)

[5] D. F. Rasheeduzzafar, A. S. Al-Gahtani, Corrosion of reinforcement in concrete structures in the Middle East [J]. Concrete International, 1985, 7(9): 48-55.

[6] Liu Guojian. Corrosion behavior and mechanism of steel reinforcement in concrete under severe composite media erosion [D]. Southeast University,2019.

[7] De Weerdt K, Justnes H. The effect of sea water on the phase assemblage of hydrated cement paste[J]. Cement and Concrete Composites, 2015, 55: 215-222.

[8] De Weerdt K, Justnes H, Geiker M R. Changes in the phase assemblage of concrete exposed to sea water[J]. Cement and Concrete Composites, 2014, 47: 53-63.

[9] X. Liu, P. Feng, W. Li, G. Geng, J. Huang, Y. Gao, S. Mu, J. Hong, Effects of pH on the nano/micro structure of calcium silicate hydrate (CSH) under sulfate attack[J]. Cement and Concrete Research, 2021, 140: 106306.

[10] J. Wang, D. Niu, Y. Wang, B. Wang, Durability performance of brine-exposed shotcrete in Salt Lake environment[J]. Construction and Building Materials, 2018, 188: 520-536.

[11] Buenfeld N R, Newman J B. The development and stability of surface layers on concrete exposed to sea-water [J]. Cement and Concrete Research, 1986, 16(5): 721-732.

ISSN: 2414-1895 DOI: 10.6919/ICJE.202306_9(6).0011

[12] Haiyan Ma, Wei Gong, Hongfa Yu, Wei Sun, Durability of concrete subjected to dry-wet cycles in various types of Salt Lake brines[J]. Construction and Building Materials, 2018, 193: 286-294.

[13] Tan Y, Yu H. Freeze–thaw durability of air-entrained concrete under various types of Salt Lake brine exposure[J]. Magazine of Concrete Research, 2018, 70(18): 928-937.

[14] Li Jianqiang. Study on ion transport and reaction in concrete in Marine corrosion Zones [D]. Qingdao University of Technology, 2016.

[15] M. Schumacher, Seawater Corrosion Handbook[M], Noyes Data Corp, New York, 1979.

[16] Brown P W, Badger S. The distributions of bound sulfates and chlorides in concrete subjected to mixed NaCl, MgSO4, Na2SO4 attack[J]. Cement and Concrete Research, 2000, 30(10): 1535-1542.

[17] Wang K, Nelsen D E, Nixon W A. Damaging effects of deicing chemicals on concrete materials[J]. Cement and concrete composites, 2006, 28(2): 173-188.

[18] P. Ghods, O. Burkan Isgor, F. Bensebaa, D. Kingston, Angle-resolved XPS study of carbon steel passivity and chloride-induced depassivation in simulated concrete pore solution[J]. Corrosion Science, 2012, 58: 159-167.

[19] Cheng S, Shui Z, Sun T, Gao X, Guo C. Effects of sulfate and magnesium ion on the chloride transportation behavior and binding capacity of Portland cement mortar[J]. Construction and Building Materials, 2019, 204: 265-275.

[20] Kunther W, Lothenbach B, Scrivener K. Influence of bicarbonate ions on the deterioration of mortar bars in sulfate solutions [J]. Cement and concrete research, 2013, 44: 77-86.